Elastomers and Composites
Vol. 53, No. 3, pp. 158~167 (September 2018)

Print ISSN 2092-9676/Online ISSN 2288-7725
DOI: https://doi.org/10.7473/EC.2018.53.3.158

Fabrication of CNT/$MgCl_2$-Supported Ti-based Ziegler-Natta Catalysts for Trans-selective Polymerization of Isoprene

Lan Cao[*,], Xiaojie Zhang[**], Xiaolei Wang[*], Chengzhong Zong[*], and Jin Kuk Kim[**,†]**

[*]*School of Polymer Science and Engineering, Qingdao University of Science and Technology, Qingdao, Shandong 266042, China*
[**]*Elastomer Lab, Department of Materials Engineering and Convergence Technology, Gyeongsang National University, Jinju 52828, Republic of Korea*

(Received September 3, 2018, 1st Revised September 16, 2018, 2nd Revised September 19, 2018, Accepted September 28, 2018)

Abstract: In this study, in-situ trans-selective polymerization of isoprene was carried out using titanium-based Ziegler–Natta catalysts. The catalysts were prepared by high-energy ball milling. Individually Large-inner-diameter carbon nanotubes (CNTL), and hydroxylated carbon nanotubes (CNTOH), along with magnesium chloride ($MgCl_2$) were used as the carriers for the catalysts. The optimum ball-milling time for preparing the CNT/$MgCl_2$/$TiCl_4$ Ziegler–Natta catalysts was 4 h. The CNTOH/$MgCl_2$/$TiCl_4$ catalyst showed a higher efficiency than that of the CNTL/$MgCl_2$/$TiCl_4$ catalyst, based on the rate of polymerization. The effects of the CNT-filler type on the isoprene polymerization behaviors and polymer properties were investigated. The morphologies of the trans-1,4-polyisoprene (TPI)/CNT and TPI/CNTOH nanocomposites exhibited a tube-like shape, and the CNTL and CNTOH fillers were well dispersed in the TPI matrix. In addition, the thermal stability of TPI significantly increased upon the introduction of a small amount of both CNTL/CNTOH fillers (0.15 wt%), owing to the satisfactory dispersion of the CNTL/CNTOH in the TPI matrix.

Keywords: Ziegler-Natta catalyst, trans-polyisoprene, carbon nanotubes, ball-milling

Introduction

As one kind of one-dimensional nanomaterial, carbon nano tube (CNT) is featured with outstanding elasticity modulus and tensile strength, preferable flexibility, small diameter and large aspect ratio, good chemical stability, electrical conductivity and thermostability etc.[1,2] Hence, CNT have a bright furture in nanocomposites such as polymers, ceramics, metal and biomaterials etc.[2-7] However, due to the strong π-π interaction between CNT, CNT can form a strong aggregation structure in matrix and difficult to disentangle and disperse in the polyolefin matrix.[8,9] Currently, lots of methods have been proposed to improve the CNT based nancomposites uniformly, such as solution mixing, emulsion mixing, melt blending and in-situ polymerization blending.[10,11] Stemming from polymerization-filling technique (PFT),[12,13] in-situ polymerization method seems to be an ideal way to realize the dispersion of fillers in polyolefin, which producing supported catalyst by loading catalyst on the surface of fillers and letting the resultant catalyst react with monomers.[14-16] Wang et al. prepared nanocomposite of Nylon-6 by in situ ring-opening polymerization have improved thermal and mechanical properties.[17] Zhang et al. applied reduced graphene oxide (rGO) supported MAO catalyst and graphene/$MgCl_2$ supported Ti-based Ziegler-Natta catalysts for vinyl polymerization and got significant improvement in mechanical properties and thermal stability of the nanocomposites.[18-20]

Various catalysts have been reported for the polymerization of isoprene, but the polymer are mainly cis 1,4-polyisoprene or 3,4-polyisoprene, and rarely have isospecific trans 1,4-selectivity.[21,22] Trans 1,4-polyisoprene (TPI) can be crystallized at room temperature because of high a regularity of main molecular chains.[23] Due to the unsaturated double bonds, it shows rubbery state after the vulcanization.[24,25] Consequently, TPI possess shape memory capability, excellent dynamic fatigue resistance capability, abrasive resistance capability etc. TPI is suitbale to be used in formulation of shape memory materials, damping product, tyre treads, toothpaste, medical splint, golf cover, etc.[26,27]

However, seldom researches introduce nanomaterials in polyisoprene through in-situ polymerization method. In the

[†]Corresponding author E-mail: rubber@gnu.ac.kr

present research, CNT/$MgCl_2$ was used as composite support and high energy ball milling method was used to in situ load Ziegler-Natta catalyst, which was further used to synthesize TPI/CNT nanocomposite. Generally speaking, the CNT composite prepared through in situ polymerization, the intermolecular interaction in CNT can be effectively weaken due to the coating effect of the molecular chains of polyisoprene to CNT, which can well prevent CNT from forming strong aggregation structure and realize the good dispersion of CNT. The CNT with the coverage of polyisoprene on the surface can well disperse in polyisoprene rubber matrix. The present research succeeded in synthesizing polyisoprene/single-walled carbon nanotube nanocomposite with CNT/$MgCl_2$ supported Ziegler-Natta catalyst, as well as a preliminary exploration of the polymerization behaviors and thermal stability properties of the nanocomposite.

Experimental

1. Materials

Hydroxylated carbon nanotubes (CNTOH) (outer diameter (OD) around 8 nm, inner diameter (ID): 2-5 nm, length: 10-30 μm) and large inner diameters carbon nanotubes (CNTL) were provided by Chengdu Organic Chemistry Co., Ltd., China. Anhydrous magnesium chloride (purity, 98%), titanium tetrachloride (purity, 99%), and isoprene (purity, 99%) were procured from Sigma-Aldrich, China. Triisobutylaluminum (TIBA) (purity, 98%) was obtained from Akzonobel, USA.

2. Preparation of CNTL/$MgCl_2$ and CNTOH/$MgCl_2$-supported Ziegler-Natta Catalysts

This section was designed to utilize ball milling to prepare the CNTOH/$MgCl_2$/$TiCl_4$ catalyst/CNTL/$MgCl_2$/$TiCl_4$ catalyst with well dispersed CNTOH/CNTL sheets. 30 g $MgCl_2$ and 10 g CNTL (CNTOH) were added into the ball-milling agate jar under nitrogen atmosphere. Keep ball milling at 500 rpm for 1 hour, the mixture turned out to be more uniform. Then, 1.18 mL $TiCl_4$ were directly added into the ball-milling agate jar under nitrogen atmosphere respectively. Hours later, the CNTL/$MgCl_2$/$TiCl_4$ (CNTOH/$MgCl_2$/$TiCl_4$) catalyst was obtained. Then, these two kinds of catalysts were applied in the isoprene polymerization.

3. Isoprene Polymerization

The polymerization was implemented in a 250 mL glass reactor filled with nitrogen to remove the moisture oxygen. 180 mL isoprene and the co-catalyst TIBA was added to the reactor then the glass reactor was placed in an ice-water mixture for the pre-polymerization (in the absence of pre-polymerization experiments, this process was abolished). After half an hour the catalyst was poured into the reactor, then pre-polymerization in the ice-water mixture for 10 minutes. After reacting at 20°C for 10 hours the polymerization was terminated by adding 10% HCl-ethanol solution, and then dried under vacuum oven at 40°C until a constant weight was achieved. The polymers obtained by the catalyst of CNTOH/$MgCl_2$/$TiCl_4$ named TPI/CNTOH and obtained by the catalyst of CNTL/$MgCl_2$ /$TiCl_4$ named TPICNTL, respectively.

4. Characterization

Fourier transform infrared spectroscopy (FTIR) of polyisoprene composites were recorded using a VERTEX 70 infrared spectrometer in the range of 400-4000 cm^{-1}. Morphologies of the catalyst and composites were examined using a scanning electron microscopy (SEM, JEM-2100F). X-ray diffraction (XRD) patterns were obtained using a Rigaku D/MAX-2500 X-ray diffractometer (Japan). Thermogravimetric analysis (TGA) was conducted using a Q800 thermal analyser (TA, America) under nitrogen atmosphere at a heating rate of 20°C/min. The weight loss was measured from 30 to 800°C.

Results and Discussion

1. Preparation of CNTL/$MgCl_2$ and CNTOH/$MgCl_2$ supported Ti-based Ziegler–Natta catalyst

The preparation of CNTL/$MgCl_2$ and CNTOH/$MgCl_2$ supported Ti-based Ziegler–Natta catalyst is illustrated in Scheme 1. In the process of preparation of the catalyst, the CNTL/$MgCl_2$ and CNTOH/$MgCl_2$-supported Ziegler-Natta catalysts were synthesized via high-energy ball milling. During this step, the surfaces of the CNTL and CNTOH were covered with $MgCl_2$-$TiCl_4$ catalyst, which prevented possible aggregation of CNT/CNT layers. The -OH group on the surfaces of CNT can interact with the surfaces of $MgCl_2$ in

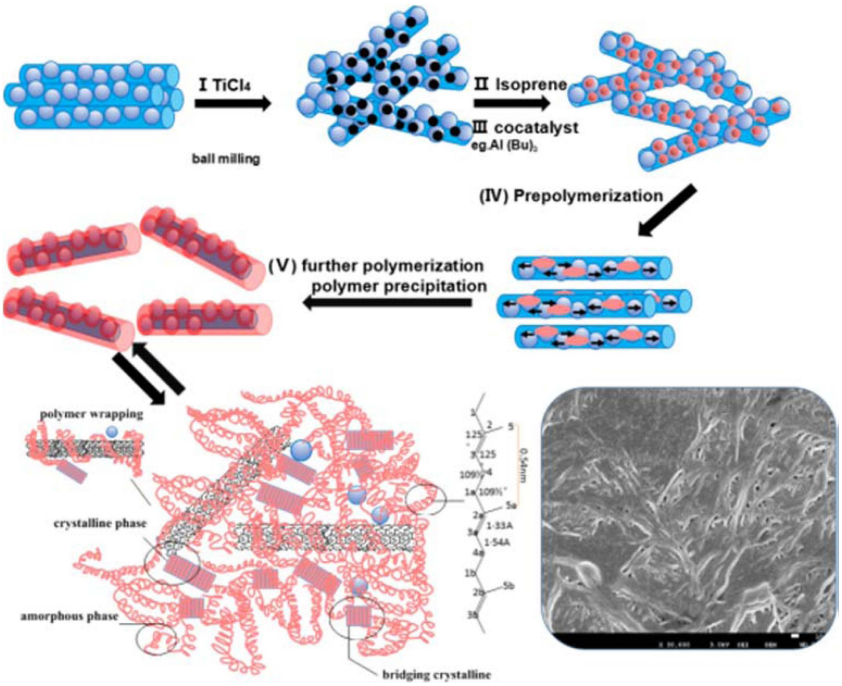

Figure 1. Schematic representation for synthesis of CNTL/$MgCl_2$/$TiCl_4$ and CNTOH/$MgCl_2$/$TiCl_4$ catalyst.

two distinct ways: by interaction of hydrogen atoms with surface chlorine atoms or via interaction of electron pairs of the oxygen with magnesium.[28] To be specific, there were three major factors preventing the aggregation of CNT/CNTOH. Firstly, $MgCl_2$ attached the surface of the CNTL and CNTOH so it can be prevented the Van der Waals force and π-π interaction. Besides, during the high-energy ball milling process, the planetary ball mill possessed greater impact, compression and shearing intensity.[29,30] The crashing effect became more intensive and the powders were mixed more uniform, which could turn $MgCl_2$ attached to the surface of CNT will have more active sites exposed to the surface, and this will be beneficial for the catalyst activity. Hence, here we have formulated CNT/$MgCl_2$ supported $TiCl_4$ based Ziegler-Natta catalyst using a solvent-free, ball milling based facile method. Subsequently, the resultant two kinds of catalysts were used during isoprene polymerization to prepare the TPI/CNTL and TPI/CNTOH nanocomposite.

1.1. Morphology Characterization of catalyst by SEM

Morphologies of the two catalysts have been compared using SEM analysis and shown in Figure 2. Figure 2(a) shows the dispersed state of CNTOH in CNTOH/$MgCl_2$/$TiCl_4$ catalyst; Figure 2(b) shows the dispersed state of CNTL in $TiCl_4$/CNT/$MgCl_2$ catalyst. As shown in these two figures, CNTOH and CNTL disentangled and dispersed uniformly in the catalysts. In the ball milling process lamella, $MgCl_2$ inserts between CNT or partially cover on the surface

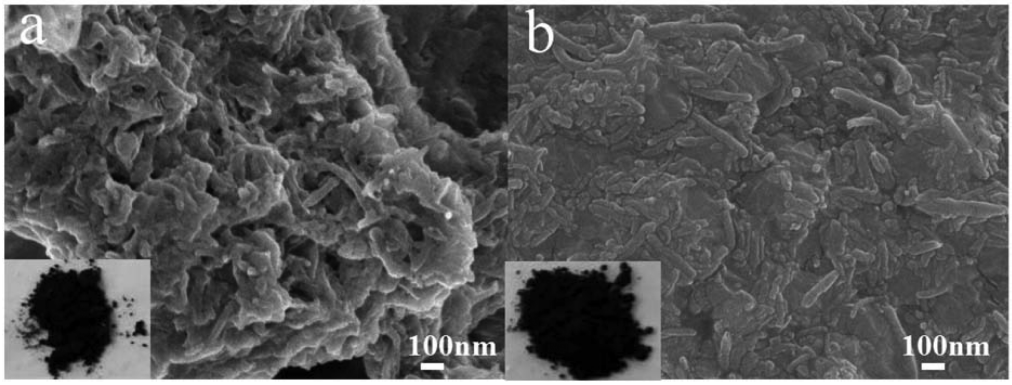

Figure 2. SEM images of (a) CNTOH in CNTOH/$MgCl_2$/$TiCl_4$ catalyst (b) CNTL in CNTL/$MgCl_2$/$TiCl_4$ catalyst.

of CNT,[19,20] which weakens the π-π interaction between CNT and thus makes CNT disentangle and disperse uniformly in the catalyst.

1.2. Influence of ball-milling time on catalytic efficiency

Figure 3 shows the catalytic efficiency of CNTL/$MgCl_2$/$TiCl_4$ and CNTOH/$MgCl_2$/$TiCl_4$ Ziegler-Natta catalysts at different milling time . After the milling time reaches 4 hours with 500 rpm, prolonging the milling time brings minor effects on the catalytic efficiency. Due to the fact that the faster revolving speed and stronger impacting, shearing, milling and compressing effects than traditional mill,[31] planetary ball mill presents obvious advantages in breaking and homogenizing powder. After a specific period, the planetary ball mill achieved a kind of balance between smashing and dispersing systems. In consideration of the energy consumption and catalytic activity, the optimum ball-milling time is 4 hours. Hence, the present research sets 4 hours as the milling time for the preparation of catalysts. At the same time, the CNTOH/$MgCl_2$/$TiCl_4$ Ziegler-Natta catalysts shows higher activity than CNTL/$MgCl_2$/$TiCl_4$ Ziegler-Natta catalysts, maybe the -OH group on the surfaces of CNT can interact with the surfaces of $MgCl_2$, so the $MgCl_2$ have higher specific surface area which may cause more titanium tetrachloride active sites to be anchored to the catalyst surface and eventually lead to an increase in catalytic efficiency.

1.3. Structure Characterization of catalyst by WAXD

To measure the activity of catalyst and the dispersed state of CNTL and CNTOH, fabrication of more active catalyst has been predicted by comparative XRD analyses of pure

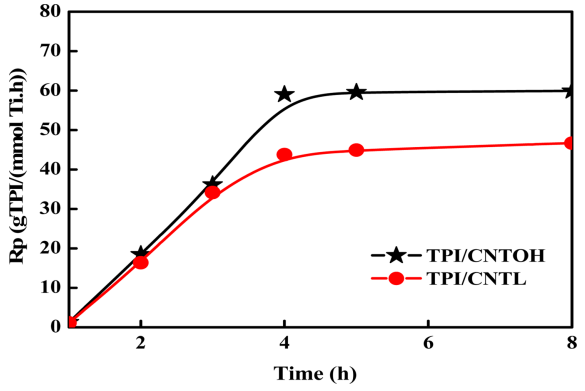

Figure 3. Rate of polymerization (Rp) using CNTL/$MgCl_2$ /$TiCl_4$ and CNTOH/$MgCl_2$ /$TiCl_4$ at different ball milling time (Rp: rate of polymerization, $Rp = \left(\frac{\text{weight of TPI (g)}}{\text{mmol of Ti}}\right)/h$.)

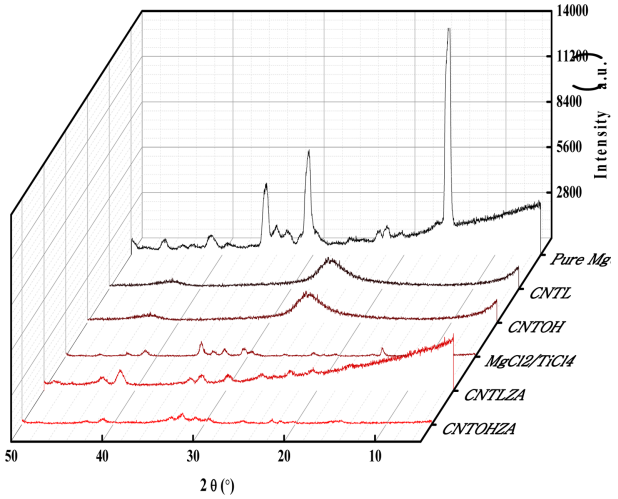

Figure 4. XRD patterns of pure $MgCl_2$ carrier, pure CNTOH carrier, pure CNTL carrier, $MgCl_2$/$TiCl_4$ catalyst, CNTL/$MgCl_2$/$TiCl_4$ and CNTOH/$MgCl_2$/$TiCl_4$ catalyst.

$MgCl_2$ carrier, pure CNT carrier, $MgCl_2$/$TiCl_4$ catalyst, CNTL/$MgCl_2$/$TiCl_4$ and CNTOH/$MgCl_2$/$TiCl_4$ catalyst. From Figure 4, in the pure $MgCl_2$ carrier curve it can be seen that high-intensity diffraction peaks are observed when 2θ is 15, 30, and 35. It means $MgCl_2$ carrier is α crystal form. When 2θ is 15, 32 and 50.5, the profile shapes of both $MgCl_2$/$TiCl_4$ catalyst and CNTOH/$MgCl_2$/$TiCl_4$ catalyst are wider at the bottom and lower at the height than the diffraction peaks of α-$MgCl_2$. The WAXD spectrogram of $MgCl_2$/$TiCl_4$ catalyst is basically same with that of CNTOH/$MgCl_2$/$TiCl_4$. It indicates that the magnesium chloride in both the prepared CNTOH/$MgCl_2$/$TiCl_4$ catalyst and $TiCl_4$/$MgCl_2$ catalyst is transferred to δ crystal of activity from the primitive α crystal. The high and steep diffraction peaks in α-$MgCl_2$ become wide and weak in δ-$MgCl_2$ of disordered structure. The reason is that the increase of δ-$MgCl_2$ of disordered structure results in the increase of content of non-crystalline parts, which increases the specific surface area of the above-mentioned Zeiger-Natta carbon nanotube catalyst; besides, the non-crystalline part of the disordered-structure $MgCl_2$ is in favor of the permeation of $TiCl_4$ into the depth. Both the increase of specific surface area and easier permeation of active component effectively increase the Ti content of carriers.

2. Polymerization of TPI/CNTOH and TPI/CNTL nanocomposites catalyzed by CNT/$MgCl_2$ supported Ti-based Ziegler–Natta catalyst

In Figure 5(a), the polymerization reaction starts at 30°C

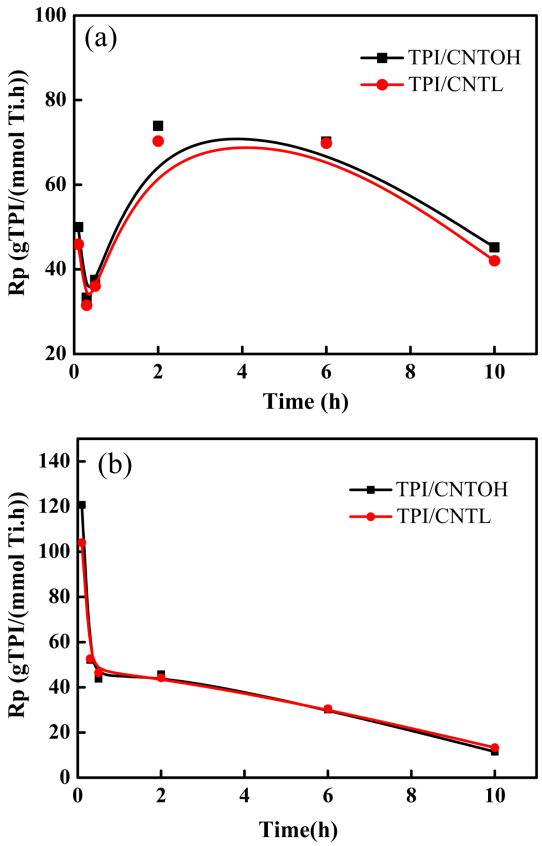

Figure 5. Rate of polymerization (Rp) using CNTL/$MgCl_2$ /$TiCl_4$ and CNTOH/$MgCl_2$/$TiCl_4$ with reaction time (a) without pre-polymerization; (b) with pre-polymerization

without pre-polymerization. Both the two kinds of catalytic activity rapidly reaches the top and then gradually declines as the reaction goes on. The possible reason is that the power-like catalyst contact monomers at a large-scale at the beginning. However, as the reaction goes on, the catalyst pieces are covered by polymer and monomers become poorer fluidity. The decrease in the catalytic activity can be attributed to the polymer of early formation functions as a physical barrier, retarding the diffusion of the isoprene into the catalyst core. With the increasement of reaction time, the rate of polymerization continuously declines till the isoprene is completely depleted.

In Figure 5(b), the polymerization reaction includes pre-polymerization in icy water for 0.5 h and then conducting polymerization reactions at 30°C. It can be seen that the catalytic activity rapidly reaches to the peak and then gradually declines during the pre-polymerization process, however, the decreasing trend was much lower than in the direct polymerization process. The possible reason is that during the beginning stage of polymerization reaction, triisobutyl aluminum deoxygenates $TiCl_4$ to $TiCl_3$ and Ti^{3+} triggers the isoprene polymerization. At the stage, the chain initiation rate and chain conversion rate are both high, so that the polymerization action presents relatively high activity. Without the pre-polymerization at low temperature, the initial polymerization rate of polyisoprene is higher than its crystallization rate (when the trans-1,4-structure is over 95%). The polymerization products possess poor formability and adhere together. While, pre-polymerization at low temperature can stabilize the active centers of catalysts, prolong catalysts' active time and effectively lower the viscidity of the system, which facilitates better morphology of polymers. During the process of polymerization, triisobutyl aluminum further deoxidizes Ti^{3+} to Ti^{2+}, which has no activity to initiate the isoprene polymerization. The foregoing mentioned reduction reaction consumes the triisobutyl aluminum. Besides, such excessive reduction reaction reduces the concentration of triisobutyl aluminum, which eventually causes the concentration reduction of catalysts active centers initiating isoprene polymerization. The catalysts present declining polymerization activity. Due to the reducing concentration of triisobutyl aluminum, the probability of polymerization active centers transferring to triisobutyl aluminum also reduces, which further reduces the chain transfer rate. As the polymerization reaction goes on for 30 minutes, chain initiation rate and chain transfer rate reach to a balanced state and catalytic active centers tend to stablilize.

Thus, the relationship of the $TiCl_4$/isoprene monomer mole ratio (shorted as n(Ti)/n(IP)) with the monomer conversion rate was studied. As shown in Figure 6, when the n(Ti)/n(IP)

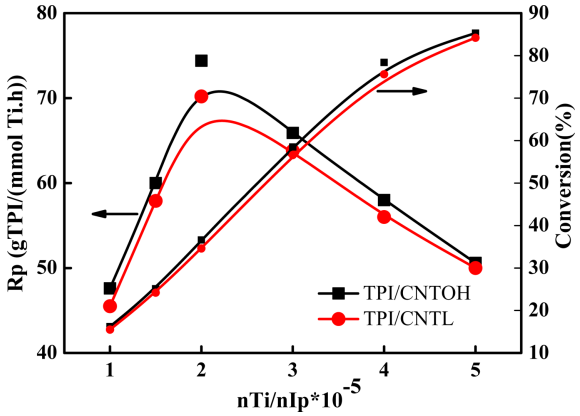

Polymerization conditions: 30°C, n(Al)/n(Ti) 70, 10 h

Figure 6. Rate of polymerization (Rp) and conversion using CNTL/$MgCl_2$/$TiCl_4$ and CNTOH/$MgCl_2$/$TiCl_4$ with different n(Ti)/n(IP)

is within the range of $1\sim5\times10^{-5}$, the monomer conversion rate increases with the increase of n(Ti)/n(IP). The reason is that when the concentration of the active component $TiCl_4$ is high, the probability that isoprene attacks $TiCl_4$ is also high. As a result, the monomer conversion rate in unit time is high. The catalytic efficiency of catalyst firstly increases and then declines with the increase of n(Ti)/n(IP) as well as reaches to the peak when the n(Ti)/n(IP) is 3.5×10^{-5}. The reason is that when the catalyst concentration is low and n(Al)/n(Ti) mole ratio reminds unchanged, the relative concentration of the cocatalyst triisobutyl aluminum in monomer is relatively low; besides, due to the active chemical characters, triisobutyl aluminum may react with some residual impurities like water and oxygen in the system, which consumes a certain amount of triisobutyl aluminum. In actual reactions, the n(Al)/n(Ti) declines and the cocatalyst triisobutyl aluminum fails to fully cause complex reaction with active centers, which lead to the declining of polymerization rate (Rp). However, after the n(Ti)/n(IP) reaches to a specific value (3.5×10^{-5}), the numbers that monomer attacks the active center relatively declines as the n(Ti)/n(IP) increases. Then the catalyst's CE calculated with unit mass of catalyst will declines. The result is consistent with relationship of CE and conversion rate gained through theoretical calculation.

As can be seen from Figure 7, the polymerization efficiency increases with the increase of Al-Ti molar ratio of Al-Ti, and the conversion rate of polymerization decreases with the increase of molar ratio of Al-Ti, which shows that the active component of the main catalyst, tetrachloro Titanium and monomer and cocatalyst triisobutyl aluminum there is the best ratio between. When the molar ratio of Al and Ti is too low, the concentration of triisobutylaluminium is too low, the triisobutylaluminum can not completely remove the impurities in the system, resulting in the loss of activity of some of the active components of the catalyst and the impurities; meanwhile, the co-catalyst The amount of triisobutylaluminium is too small, the main active component of titanium tetrachloride can not be fully coordinated with the reaction and can not form a sufficient number of active reaction centers; and when the the molar ratio of aluminum-titanium molar ratio is too high, the cocatalyst may be the main catalyst Over-reduction of titanium tetrachloride to inactive titanium dichloride will also lead to a decrease in the conversion of isoprene in the polymerized monomer. Meanwhile, an excessive amount of triisobutylaluminium will also be present in the subsequent reaction of the catalytic system Chain transfer, which is equivalent to reducing the number of active centers during the actual reaction, may also result in a decrease in the conversion of the isoprene monomer. In the catalyst system, when the ratio of aluminum to titanium is 80, the catalytic efficiency and the conversion rate achieve the optimal ratio.

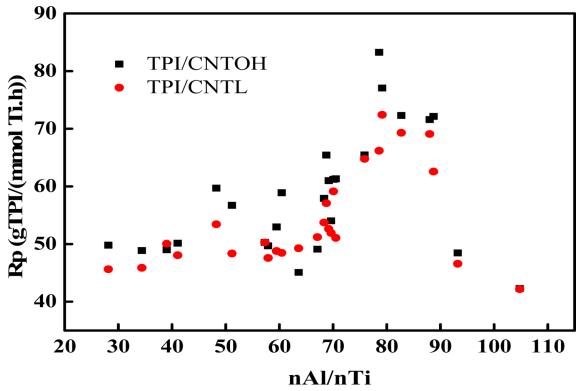

Polymerization conditions: 30°C, 10 h

Figure 7. Rate of polymerization (Rp) and conversion using CNTL/$MgCl_2$/$TiCl_4$ and CNTOH/$MgCl_2$/$TiCl_4$ with different n(Al)/n(Ti)

2.1. The structural characteristics of TPI/CNT nanocomposites by FTIR

As shown in Figure 8(a) and (b), when n(Al)/n(Ti) increases from 30 to 80, in fingerprint region, no obvious changes is observed to the peak shape of polyisoprene carbon nanotube

Table 1. Characteristic Bands of Characteristic Groups of NR and EU Gum.

Characteristic groups	Characteristic bands	
	NR (Natural rubber)	EU gum (Eucommia rubber)
-C=C-	1645 cm^{-1}	1645 cm^{-1}
$-CH_3$, $-CH_2-$	1450 cm^{-1}, 1380 cm^{-1}	1450 cm^{-1}, 1380 cm^{-1}
$-CH_2-C(CH_3)=CH-CH_2-$	835 cm^{-1}	845 cm^{-1}
Crystalline peaks		875 cm^{-1}, 798 cm^{-1}, 758 cm^{-1}, 595 cm^{-1}, 465 cm^{-1}
Configuation	cis	trans

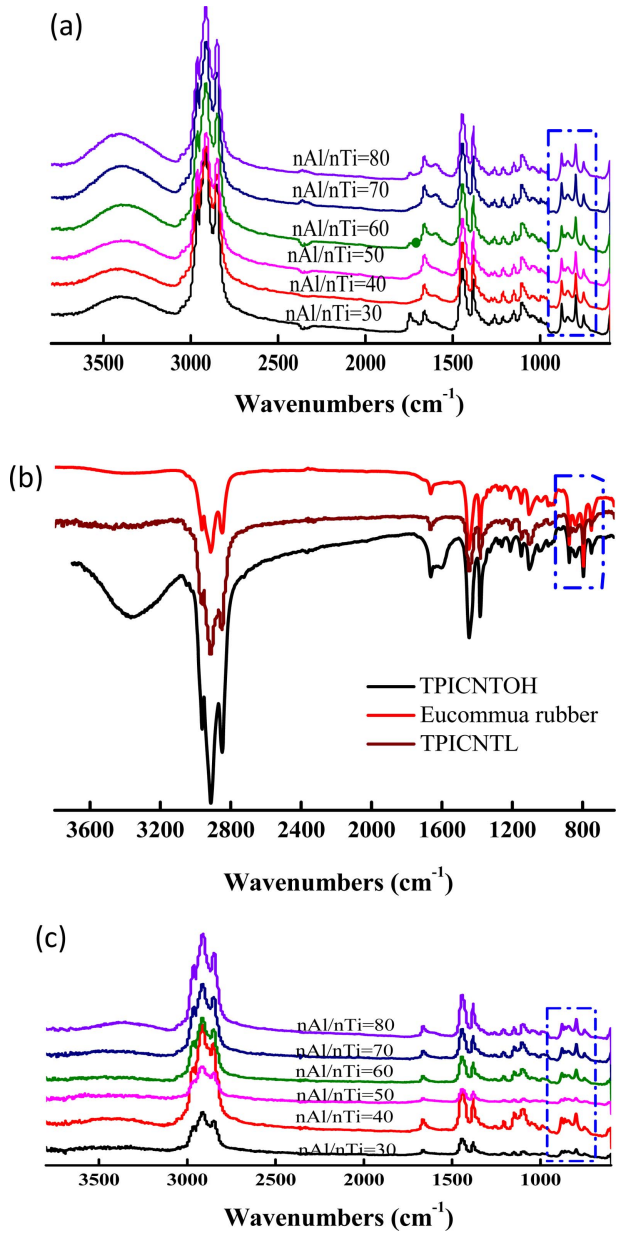

Figure 8. FTIR spectra of (a) TPI/CNTOH nanocomposites; (b) TPI/CNTL nanocomposites with different n(Al)/n(Ti); (c) TPI/CNTOH, TPI/CNTL nanocomposites and natural eucommia rubber.

composite. Thus, it can be confirmed that the changes in both n(Al)/n(Ti) and n(Ti)/n(IP) will not lead to structural changes of polyisoprene carbon nanotube composite under catalytic system. At the same time, the structure of these TPI/CNTOH and TPI/CNTL nanocomposites is close to that of natural eucommia rubber, and therefore all of them belong to trans-1,4-polyisoprene, as shown in Figure 8(c). According to the reference (Table 1),[32] the signals at 910 cm^{-1} due to the 1,2-units and the signals at 890 cm^{-1} due to the 3,4-units, which is not appear in the FTIR spectra. So here there is only contains trans 3,4-units. Then we speculated on the possible mechanism of this reaction, as shown in Figure 9.

2.2. The morphology characteristics of TPI/CNT nanocomposites by SEM

According to the morphology replication characteristics of the supported Ziegler–Natta catalyst, the morphology of the final polymer can be controlled by modifying the morphology of the catalyst.[14,16] Therefore, the morphology of the resultant TPI, TPI/CNTOH nanocomposites and TPI/CNTL nanocomposites directly mirror that of the catalyst. As shown in Figure 9, the particles of TPI obtained using the $MgCl_2$/$TiCl_4$ catalyst are white and irregularly shaped, while those of TPI/CNTOH nanocomposites and TPI/CNTL nanocomposites have a flake shape with homogeneous black color. Additionally, no high-contrast black CNTL or CNTOH sheets could be observed. Because the active points of catalysts closely contact CNT, polyisoprene molecular chains densely cover the CNT during the polymerization. Observing the polyisoprene/CNT nanocomposite, as shown in Figure 9(a) and (b), we can see that polyisoprene molecular chains cover on the surface of single-beam CNT. The polyisoprene molecular chains and single-beam CNT form a near core-shell tubular structure. Polyisoprene molecular chains grow during the polymerization process, get rid of active centers and produce crystallization growth near the surface of CNT. Because the active centers disperse uniformly, uniform polyisoprene crystals are formed on the surface of CNT, featuring morphologic reproduction effect and well demonstrating the morphology of CNT.

2.3. The thermal stability characteristics of TPI/CNT nanocomposites by TGA

As shown in Figure 10, Compared with pure polyisoprene, as the nanotube content increases, the highest temperature at thermal weight loss is increased from 380°C to 402°C. The obvious improvement in thermal stability is related to the network structure of the composite and seldom relates to the types of CNT.

Conclusion

The large inner diameters carbon nanotubes (CNTL), hydroxylated carbon nanotubes (CNTOH) and magnesium chloride ($MgCl_2$) were used as the carriers for the Titanium-based Ziegler-Natta catalyst, which achieved well dispersion

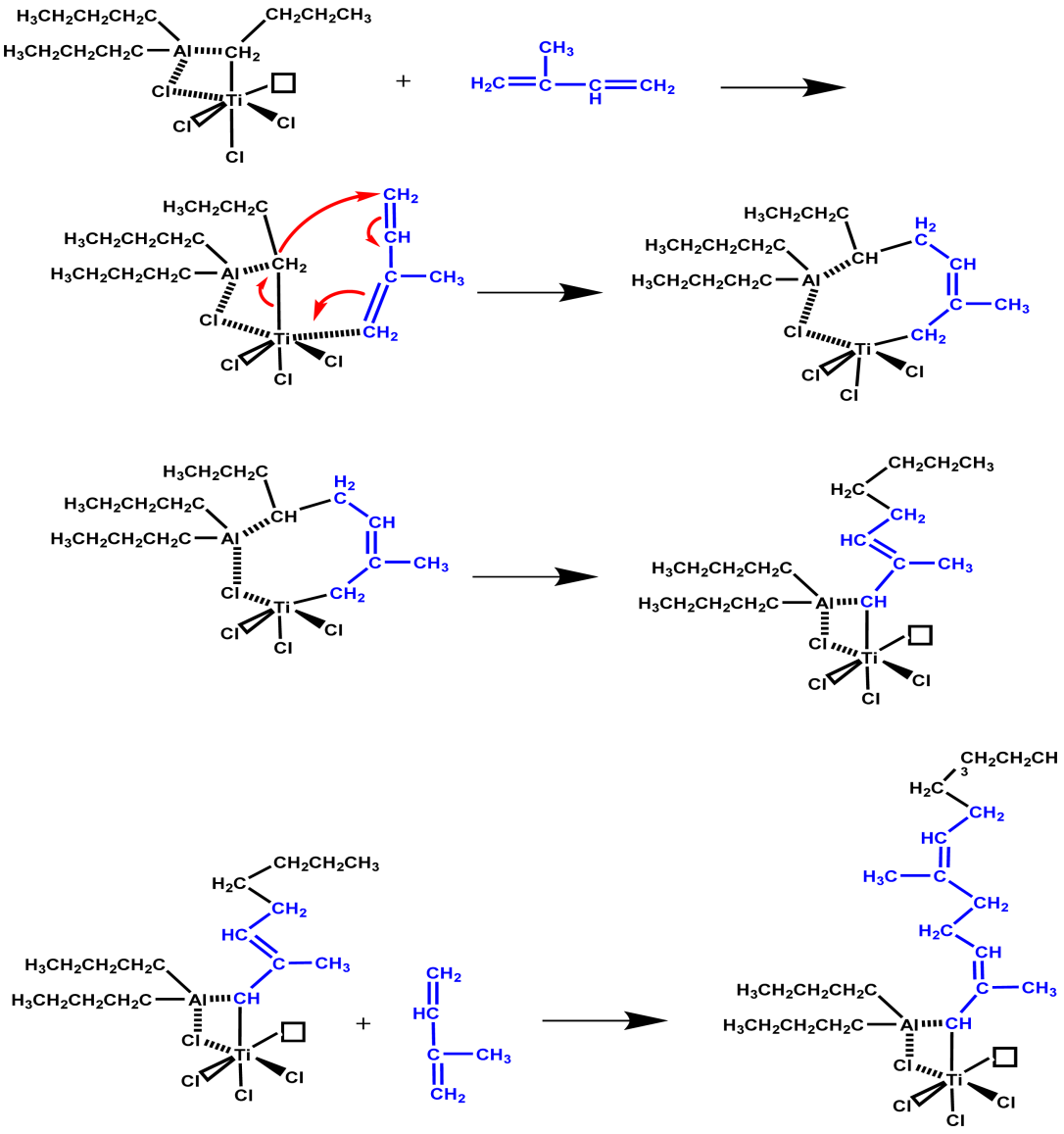

Figure 9. Mechanism of isoprene $TiCl_4/MgCl_2$-Al(i-Bu)$_3$ system.

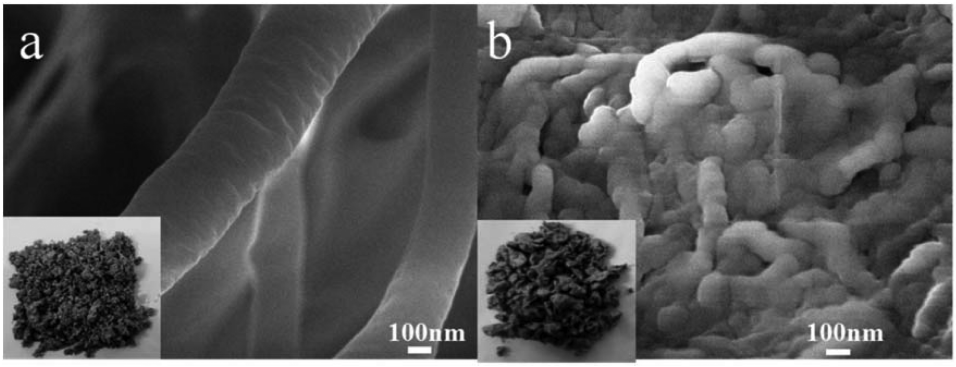

Figure 10. SEM images of (a)TPI/CNTOH nanocomposites and (b) TPI/CNTL nanocomposites.

by the high-energy ball-milling technique. The optimum ball-milling time for preparing CNT/$MgCl_2$/$TiCl_4$ Ziegler-Natta catalysts was 4 hours. The polymerization rate turned out that CNTOH/$MgCl_2$/$TiCl_4$ Ziegler-Natta catalysts has higher

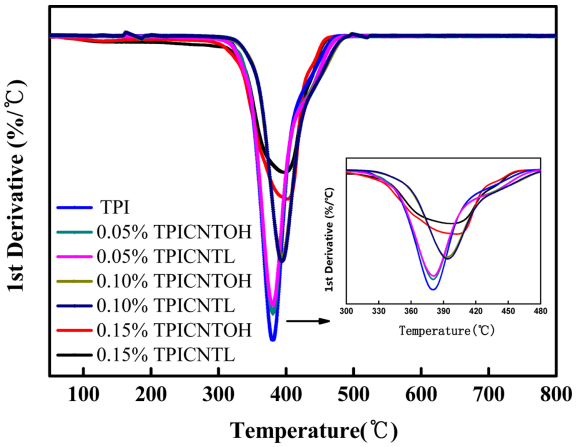

Figure 11. The TGA 1st Derivative curves of TPI/CNTOH nanocomposites and TPI/CNTL nanocomposites with Mw ≈ 420~460 k. Insert: magnified TGA curves from 25°C to 800°C.

efficiency. Meanwhile, TPI/CNT and TPI/CNTOH nanocomposites was synthesized by in-situ trans-selective polymerization with CNT/$MgCl_2$ supported Ziegler-Natta catalyst. The morphologies of the TPI/CNT and TPI/CNTOH nanocomposites exhibited a tube-like shape and the CNTL and CNTOH fillers were well dispersed in the TPI matrix. In addition, the thermal stability properties of the TPI were significantly enhanced by the CNTL/CNTOH fillers (0.15 wt%).

Acknowledgement

This work was supported by the Natural Science Foundation of Shandong Province (project No.: ZR2016XJ002), Republic of China and the Materials, and Components Technology Development Program of MOTIE/KEIT. [10067683, Development of Manufacturing Technology of High Barrier Elatomeric Material] of Korea.

References

1. S. Iijima, "Helical microtubules of graphitic carbon", *Nature*, **354**, 56 (1991).
2. F. H. Gojny, J. Nastalczyk, Z. Roslaniec, and K. Schulte, "Surface modified multi-walled carbon nanotubes in CNT/epoxy-composites", *Chem. Phy. Lett.*, **370**, 820 (2003).
3. M. H. Al-Saleh and U. Sundararaj, "Electromagnetic interference shielding mechanisms of CNT/polymer composites", *Carbon*, **47**, 1738 (2009).
4. W. A. Curtin and B. W. Sheldon, "CNT-reinforced ceramics and metals", *Mater. Today*, **7**, 44 (2004).
5. N. Saito, Y. Usui, K. Aoki, N. Narita, M. Shimizu, N. Ogiwara, K. Nakamura, N. Ishigaki, H. Kato, and S. Taruta, "Carbon nanotubes for biomaterials in contact with bone", *Curr. Med. Chem.*, **15**, 523 (2008).
6. A. A. Koval'chuk, V. G. Shevchenko, A. N. Shchegolikhin, P. M. Nedorezova, A. N. Klyamkina, and A. M. Aladyshev, "Effect of carbon nanotube functionalization on the structural and mechanical properties of polypropylene/MWCNT composites", *Macromolecules*, **41**, 7536 (2008).
7. P. Rossi, S. Suarez, F. Soldera, and F. Mücklich, "Quantitative Assessment of the Reinforcement Distribution Homogeneity in CNT/Metal Composites", *Adv. Eng. Mater.*, **17**, 1017 (2015).
8. Y. Han, X. Zhang, X. Yu, J. Zhao, S. Li, F. Liu, P. Gao, Y. Zhang, T. Zhao, and Q. Li, "Bio-inspired aggregation control of carbon nanotubes for ultra-strong composites", *Sci. REP-UK*, **5**, 11533 (2015).
9. G. Kozlov, Z. Zhirikova, V. Aloev, and G. Zaikov, "The ultrasound processing influence on carbon nanotubes structure in polymer nanocomposites", *Chem. Chem. Technol.*, **8**, 57 (2014).
10. G. Mittal, V. Dhand, K. Y. Rhee, S.-J. Park, and W. R. Lee, "A review on carbon nanotubes and graphene as fillers in reinforced polymer nanocomposites", *J. Ind. Eng. Chem.*, **21**, 11 (2015).
11. M. L. Bhaisare, M. S. Khan, S. Pandey, G. Gedda, and H.-F. Wu, "Shape-oriented photodynamic therapy of cuprous oxide (Cu_2O) nanocrystals for cancer treatment", *RSC Adv.*, **7**, 23607 (2017).
12. F. D. C. Fim, J. M. Guterres, N. R. Basso, and G. B. Galland, "Polyethylene/graphite nanocomposites obtained by in situ polymerization", *J. Polym. Sci. Pol. Chem.*, **48**, 692 (2010).
13. M. Alexandre, M. Pluta, P. Dubois, and R. Jérôme, "Metallocene catalyzed polymerization of ethylene in the presence of graphite, 1. Synthesis and characterization of the composites", *Macromol. Chem. Phys.*, **202**, 2239 (2001).
14. W. Kaminsky and K. Wiemann, "Polypropene nanocomposites by metallocene/MAO catalysts", *Compos.*, **13**, 365 (2006).
15. D. Bonduel, S. Bredeau, M. Alexandre, F. Monteverde, and P. Dubois, "Supported metallocene catalysis as an efficient tool for the preparation of polyethylene/carbon nanotube nanocomposites: effect of the catalytic system on the coating morphology", *J. Mater. Chem.*, **17**, 2359 (2007).
16. W. Kaminsky, A. Funck, "In Situ Polymerization of Olefins with Nanoparticles by Metallocene-Catalysis", in: *Macromol. Symp.*, **260**, 1 (2007).
17. X. Wang, E. N. Kalali, and D.-Y. Wang, "An in situ polymerization approach for functionalized MoS_2/nylon-6 nanocomposites with enhanced mechanical properties and thermal

stability", *J. Mater. Chem. A*, **3**, 24112 (2015).
18. H. Zhang, J.-H. Park, Y.-K. Moon, E.-B. Ko, D.-h. Lee, Y. Hu, X. Zhang, and K.-B. Yoon, "Preparation of graphene/$MgCl_2$-supported Ti-based Ziegler-Natta catalysts by the coagglomeration method and their application in ethylene polymerization", *Chinese J. Catal.*, **38**, 131 (2017).
19. H.-X. Zhang, J.-H. Park, E.-B. Ko, Y.-K. Moon, D.-h. Lee, Y.-M. Hu, X.-Q. Zhang, and K.-B. Yoon, "Comparison of the properties of graphene-and graphene oxide-based polyethylene nanocomposites prepared by an in situ polymerization method", *RSC Adv.*, **6**, 73013 (2016).
20. H.-x. Zhang, J.-H. Park, and K.-B. Yoon, "Excellent electrically conductive PE/rGO nanocomposites: In situ polymerization using rGO-Supported MAO cocatalysts", *Compos. Sci. Technol.*, **154**, 85 (2018).
21. G. Natta, L. Porri, and A. Carbonaro, "Polymerization of conjugated diolefins by homogeneous aluminum alkyl-titanium alkoxide catalyst systems. II. 1,2-polybutadiene and 3,4-polyisoprene", *Macromol. Chem. Phys.*, **77**, 126 (1964).
22. L. Zhang, Y. Luo, and Z. Hou, "Unprecedented isospecific 3, 4-polymerization of isoprene by cationic rare earth metal alkyl species resulting from a binuclear precursor", *J. Am. Chem. Soc.*, **127**, 14563 (2005).
23. C. Bunn, "Molecular structure and rubber-like elasticity II. The stereochemistry of chain polymers", *Proc. R. Soc. Lond. A*, **180**, 67 (1942).
24. A. Shanmugharaj, J. Bae, K. Y. Lee, W. H. Noh, S. H. Lee, and S. H. Ryu, "Physical and chemical characteristics of multiwalled carbon nanotubes functionalized with aminosilane and its influence on the properties of natural rubber composites", *Compos. Sci. Technol.*, **67**, 1813 (2007).
25. E. Kent and F. Swinney, "Properties and applications of trans-1,4-polyisoprene", *Ind. Eng. Chem. Res.*, **5**, 134 (1966).
26. R. Jones and Y. Wei, "Application of trans-1, 4 polyisoprene in orthopedic and rehabilitation medicine", *J. Biomed. Mater. Res. A*, **5**, 19 (1971).
27. G. Y. Lin, S. M. Liu, and F. C. Dong, "Study on shape-memory mechanism and properties of NR/TPI blends", *Applied Mechanics and Materials*, **467**, 146 (2014).
28. N. Bahri-Laleh, "Interaction of different poisons with $MgCl_2$/TiCl4 based Ziegler-Natta catalysts", *Appl. Surf. Sci.*, **379**, 395 (2016).
29. H. Wu, W. Zhao, H. Hu, and G. Chen, "One-step in situ ball milling synthesis of polymer-functionalized graphene nanocomposites", *J. Mater. Chem.*, **21**, 8626 (2011).
30. W. Zhao, M. Fang, F. Wu, H. Wu, L. Wang, and G. Chen, "Preparation of graphene by exfoliation of graphite using wet ball milling", *J. Mater. Chem.*, **20**, 5817 (2010).
31. C. De Rosa, F. Auriemma, O. Tarallo, R. Di Girolamo, E. M. Troisi, S. Esposito, D. Liguori, F. Piemontesi, G. Vitale, and G. Morini, "Tailoring the properties of polypropylene in the polymerization reactor using polymeric nucleating agents as prepolymers on the Ziegler–Natta catalyst granule", *Polym. Chem-UK*, **8**, 655 (2017).
32. G. Liu, X. Zhang, T. Zhang, J. Zhang, P. Zhang, and W. Wang. "Determination of the content of Eucommia ulmoides gum by Variable Temperature Fourier Transform Infrared Spectrum", *Polymer Testing*, **63**, 582 (2017).